

# Calcium Currents Are Enhanced by $\alpha_2\delta$ -1 Lacking Its Membrane Anchor<sup>\*[5]</sup>

Received for publication, May 4, 2012, and in revised form, July 30, 2012. Published, JBC Papers in Press, August 6, 2012, DOI 10.1074/jbc.M112.378554

Ivan Kadurin<sup>1</sup>, Anita Alvarez-Laviada<sup>2</sup>, Shu Fun Josephine Ng, Ryan Walker-Gray, Marianna D'Arco, Michael G. Fadel, Wendy S. Pratt, and Annette C. Dolphin<sup>3</sup>

From the Department of Neuroscience, Physiology and Pharmacology, University College London, Gower St., London WC1E 6BT, United Kingdom

**Background:** We examined the role of membrane anchoring of voltage-gated calcium channel  $\alpha_2\delta$  subunits.

**Results:** We used a truncated  $\alpha_2\delta$ -1 construct ( $\alpha_2\delta$ -1 $\Delta$ C-term), which still increases  $\text{Ca}_v2.1/\beta 1b$  currents, despite being mainly secreted.

**Conclusion:** The effect of  $\alpha_2\delta$ -1 $\Delta$ C-term on calcium currents does not involve secretion and subsequent re-binding to the plasma membrane.

**Significance:** C-terminal membrane anchoring of  $\alpha_2\delta$  is not essential for calcium current enhancement.

The accessory  $\alpha_2\delta$  subunits of voltage-gated calcium channels are membrane-anchored proteins, which are highly glycosylated, possess multiple disulfide bonds, and are post-translationally cleaved into  $\alpha_2$  and  $\delta$ . All  $\alpha_2\delta$  subunits have a C-terminal hydrophobic, potentially trans-membrane domain and were described as type I transmembrane proteins, but we found evidence that they can be glycosylphosphatidylinositol-anchored. To probe further the function of membrane anchoring in  $\alpha_2\delta$  subunits, we have now examined the properties of  $\alpha_2\delta$ -1 constructs truncated at their putative glycosylphosphatidylinositol anchor site, located before the C-terminal hydrophobic domain ( $\alpha_2\delta$ -1 $\Delta$ C-term). We find that the majority of  $\alpha_2\delta$ -1 $\Delta$ C-term is soluble and secreted into the medium, but unexpectedly, some of the protein remains associated with detergent-resistant membranes, also termed lipid rafts, and is extrinsically bound to the plasma membrane. Furthermore, heterologous co-expression of  $\alpha_2\delta$ -1 $\Delta$ C-term with  $\text{Ca}_v2.1/\beta 1b$  results in a substantial enhancement of the calcium channel currents, albeit less than that produced by wild-type  $\alpha_2\delta$ -1. These results call into question the role of membrane anchoring of  $\alpha_2\delta$  subunits for calcium current enhancement.

age-activated channels, the  $\alpha 1$  subunit is associated with an intracellular  $\beta$  subunit, which is required for the channel to reach the plasma membrane (2–4), and an  $\alpha_2\delta$  subunit, whose functions are less well understood but which also influences trafficking of the channel (5–7). Genes encoding 10  $\alpha 1$ , four  $\beta$ , and four  $\alpha_2\delta$  subunits have been identified (1, 8, 9).

The topology of the  $\alpha_2\delta$  protein was initially determined for skeletal muscle  $\alpha_2\delta$ -1 but is likely to generalize to all  $\alpha_2\delta$  subunits (10, 11). The  $\alpha_2\delta$  subunits were predicted to be type I transmembrane proteins, as they have an N-terminal signal peptide sequence and a C-terminal hydrophobic and potentially transmembrane region (12). From the early studies of  $\alpha_2\delta$ -1 purified from skeletal and cardiac muscle, it was identified that the  $\alpha_2$  subunit is disulfide-bonded to a transmembrane  $\delta$  subunit (13). However, both subunits are the product of a single gene, encoding the  $\alpha_2\delta$  protein, which is post-translationally glycosylated and further processed with the formation of disulfide bond(s) and subsequent proteolytic cleavage into  $\alpha_2$  and  $\delta$  (12).

In terms of function, the  $\alpha_2$  moiety of  $\alpha_2\delta$  was found to play a role in enhancement of calcium currents (11), and we showed that the von Willebrand factor-A domain in  $\alpha_2$  is essential for its trafficking function (6, 14). In contrast, the transmembrane  $\delta$  subunit was reported to function by modifying the voltage-dependent properties of the channels (10, 11).

We have recently obtained evidence that  $\alpha_2\delta$  subunits can form GPI-anchored proteins (15). In this study, we wished to further examine the role of membrane anchoring of  $\alpha_2\delta$ -1 by creating an anchorless  $\alpha_2\delta$ -1, truncated at the putative GPI-anchor  $\omega$ -site, which removes the C-terminal hydrophobic domain (Fig. 1,  $\alpha_2\delta$ -1 $\Delta$ C-term, *construct iii*). A similar approach has been taken with GPI-anchored prion protein, which was found to remain associated with lipid rafts despite the loss of membrane anchoring (16). The interaction of a transmembrane form of prion protein with lipid rafts was found to require interaction with glypicans, which are themselves GPI-anchored (17).

We have examined the role of membrane anchoring of  $\alpha_2\delta$ -1 on its biochemical properties, processing, subcellular localiza-

Voltage-gated  $\text{Ca}^{2+}$  ( $\text{Ca}_v$ )<sup>4</sup> channels comprise an  $\alpha 1$  subunit, which forms the pore and determines the main functional and pharmacological attributes of the channel (1). For the high volt-

\* This work was supported in part by Medical Research Council Grants G0700368 and G0801756.

Author's Choice—Final version full access.

[5] This article contains supplemental Figs. 1 and 2.

<sup>1</sup> To whom correspondence may be addressed. Tel.: 44-2076793276; Fax: 44-2076790042; E-mail: i.kadurin@ucl.ac.uk.

<sup>2</sup> Supported by a Biotechnology and Biological Sciences Research Council studentship.

<sup>3</sup> To whom correspondence may be addressed. Tel.: 44-2076793276; Fax: 44-2076790042; E-mail: a.dolphin@ucl.ac.uk.

<sup>4</sup> The abbreviations used are:  $\text{Ca}_v$ , voltage-gated calcium; Ab, antibody; DRG, dorsal root ganglion; DRM, detergent-resistant membrane; GPI, glycosylphosphatidylinositol; PNGase, peptide N-glycosidase; WCL, whole cell lysate; BisTris, 2-[bis(2-hydroxyethyl)amino]-2-(hydroxymethyl)propane-1,3-diol; CFP, cyan fluorescent protein.

tion, and function. We present the surprising evidence that  $\alpha_2\delta$ -1 $\Delta$ C-term is still able to produce a significant enhancement of  $\text{Ca}_v2.1/\beta 1b$  calcium channel currents following its heterologous expression, indicating that intrinsic membrane anchoring is not essential for this property. Furthermore, we have found that although a large fraction ( $\sim 75\%$  after 3 days in culture) of  $\alpha_2\delta$ -1 $\Delta$ C-term is soluble and secreted into the medium, some of this protein remains extrinsically associated with the external leaflet of the plasma membrane. Future studies will be directed toward identifying the binding partner(s) of  $\alpha_2\delta$ -1 $\Delta$ C-term mediating this extrinsic interaction.

## EXPERIMENTAL PROCEDURES

**Molecular Biology**— $\alpha_2\delta$ -1 $\Delta$ C-term was constructed with a C-terminal HA tag, followed immediately by a STOP codon inserted directly after Cys-1059 (thus abolishing the Cys-1059/Gly-1060/Gly-1061-predicted GPI anchor  $\omega$ -site). A second construct was made with an HA tag between Asn-549 and Asp-550, which was also truncated by a STOP codon immediately after Cys-1059. All mutations were made by standard molecular biological techniques and verified by DNA sequencing.

**Heterologous Expression of cDNAs**—The calcium channel cDNAs used were rabbit  $\text{Ca}_v2.1$  (M64373), rat  $\alpha_2\delta$ -1 (M86621), and rat  $\beta 1b$  (18). The cDNAs were cloned into the pMT2 vector for expression, unless otherwise stated. tsA-201 cells were transfected with the cDNA combinations stated. The cDNA for green fluorescent protein (mut3 GFP) (19) was also included to identify transfected cells from which electrophysiological recordings were made. Transfection was performed as described previously (20). In control experiments where  $\alpha_2\delta$  was omitted, the ratio was made up as stated with empty vector.

**Dorsal Root Ganglion (DRG) Neuron Culture and Transfection**—DRG neurons were isolated from P10 Sprague-Dawley rats and transfected by Amaxa nucleofection as described in the manufacturer's protocol (program G13, Lonza). Briefly, neurons were dissociated in dissection solution as follows: Hanks' basal salt solution buffer containing 5 mg/ml Dispase (Invitrogen), 2 mg/ml collagenase type 1A (Worthington), and 0.1 mg/ml DNase, (Invitrogen), for 30 min at 37 °C, and then resuspended in 160  $\mu$ l of nucleofection buffer (80  $\mu$ l per sample). 2  $\mu$ g of total plasmid DNA was used for each transfection condition. For expression,  $\alpha_2\delta$ -1 mid-HA and  $\alpha_2\delta$ -1 $\Delta$ C-term-HA were used in pcDNA3. Enhanced cyan fluorescent protein (Clontech) was co-transfected with  $\alpha_2\delta$ -1 cDNA at a ratio of 1:4. After transfection, DRGs were plated on poly-L-lysine-coated glass coverslips and cultured in DMEM/F-12 medium (Invitrogen) supplemented with 10% FBS and 50 ng/ml NGF. Culture medium was replaced 18 h after transfection.

**Primary Antibodies (Abs)**—The following primary Abs were used: anti- $\alpha_2$ -1 (mouse monoclonal, Sigma); anti-HA (rabbit polyclonal, Sigma, or rat monoclonal, Roche Applied Science); anti-flotillin-1 (mouse monoclonal, BD Biosciences); anti-Akt/PKB (rabbit polyclonal, Cell Signaling Technologies), and anti-GAPDH (mouse monoclonal, Ambion).

**Cell Lysis, Cell Surface Biotinylation, and Immunoblotting**—The procedures were modified from those described previously (15, 20). 72 h after transfection, tsA-201 cells were rinsed with

phosphate-buffered saline (PBS, pH 7.4, Sigma) and then incubated with PBS containing 1 mg/ml EZ-link Sulfo-NHS-LC-Biotin (Thermo Scientific) for 30 min at room temperature. Cells were then rinsed twice with PBS containing 200 mM glycine to quench the reaction. The cells were scraped, resuspended in cold PBS, and centrifuged at 1000  $\times$  g at 4 °C for 10 min. The cell pellets were homogenized in PBS, pH 7.4, at 4 °C containing 1% Igepal and protease inhibitors (complete, Roche Applied Science) by five passes through a 23-gauge needle, followed by sonication for 10 s, and were incubated on ice for 45 min. The whole cell lysates (WCL) were then centrifuged at 20,000  $\times$  g for 25 min at 4 °C, and the pellet was discarded. Aliquots of supernatant were assayed for total protein (Bradford assay, Bio-Rad). WCL corresponding to 20–40  $\mu$ g of total protein was diluted with Laemmli sample buffer (15) supplemented with 100 mM dithiothreitol, incubated at 60 °C for 10 min, resolved by SDS-PAGE on 3–8% Tris-acetate or 4–12% Bis-Tris gels (Invitrogen), and transferred to polyvinylidene fluoride (PVDF) membrane (Bio-Rad) by Western blotting (semi-dry, Bio-Rad). 500  $\mu$ g of the same lysate was used to precipitate biotinylated protein by adding 50  $\mu$ l of prewashed streptavidin-agarose beads (Thermo Scientific) and overnight incubation at 4 °C. The beads were washed five times with PBS containing 0.1% Igepal and resuspended in an equal volume of 2 $\times$  Laemmli buffer with 100 mM DTT, followed by 10 min of incubation at 60 °C. The eluted protein was analyzed by immunoblotting, as described above. The following secondary Abs were used for Western blot: goat anti-rabbit coupled to horseradish peroxidase (HRP) and goat anti-mouse coupled to HRP (Bio-Rad). The signal was obtained by HRP reaction with fluorescent product (ECL Plus, GE Healthcare), and membranes were scanned on a Typhoon 9410 phosphorimager (GE Healthcare).

**Quantification of Western Blots**—ImageJ software (rsb.info.nih.gov) was used to draw a box around each band of interest, to quantify the mean gray intensity. The background was subtracted using an equally sized "background" box next to each band. To quantify the cleavage of  $\alpha_2\delta$  to  $\alpha_2$  and  $\delta$ , the  $\alpha_2\delta$ -1 and  $\alpha_2$ -1 bands were summed (total = cleaved + uncleaved), from which the % cleavage was calculated.

The proportion of  $\alpha_2\delta$ -1 $\Delta$ C-term-HA secreted into the medium 72 h after transfection of tsA-201 cells was quantified by measuring the mean intensity of  $\alpha_2\delta$ -1-associated bands detected by HA Ab in the media and in the WCL. Taking into account the total volume of the media and the WCL for each condition, an estimate of the amount of  $\alpha_2\delta$ -1 $\Delta$ C-term-HA protein in each fraction was obtained and expressed as % of the total  $\alpha_2\delta$ -1 $\Delta$ C-term-HA in all fractions.

**Deglycosylation with Peptide N-Glycosidase-F (PNGase-F)**—WCL were brought to 0.2–0.5 mg/ml protein in PNGase-F buffer (PBS, pH 7.4, supplemented with 75 mM  $\beta$ -mercaptoethanol, 0.5% Triton X-100, 0.1% SDS, and protease inhibitors). 1 unit of PNGase-F (Roche Applied Science) was added per 10- $\mu$ l volume and incubated at 37 °C for 5–12 h.

For the secreted proteins, equal amounts of concentrated media were taken for each reaction. For PNGase-F deglycosylation, the concentrated media were diluted with 9 volumes of PNGase-F buffer and incubated with PNGase-F as described above. Samples without enzyme were incubated in parallel in

## Anchorless $\alpha_2\delta$ -1 Enhances Calcium Currents

both cases, and the whole reaction volume was analyzed by Western blot.

**Collection of Medium**—tsA-201 cells were incubated for 72 h post-transfection, and medium was collected and centrifuged ( $1000 \times g$ ) to remove any detached cells. The supernatant was filtered through a  $0.22\text{-}\mu\text{m}$  syringe filter (Millipore). The resulting cell-free medium was applied to 3-kDa cutoff filtration column (Amicon) and centrifuged to concentrate the proteins ( $\sim 150$ -fold). Aliquots of the concentrate were diluted in the appropriate amount of Laemmli sample buffer and analyzed by Western blot.

**Preparation of Triton X-100-insoluble Membrane Fractions (DRMs)**—All steps were performed on ice. Confluent tsA-201 cells from two  $175\text{-cm}^2$  flasks were taken up in Mes-buffered saline (MBS, 25 mM Mes, pH 6.5, 150 mM NaCl, and complete protease inhibitor mixture (Roche Applied Science)) containing 1% (v/v) Triton X-100 (Thermo Scientific), resuspended by 10 passages through a 1-ml Gilson pipette tip, and left on ice for 1 h. An equal volume of 90% (w/v) sucrose in MBS was then added. The sample was transferred to a 13-ml ultracentrifuge tube and overlaid with 10 ml of discontinuous sucrose gradient, consisting of 35% (w/v) sucrose in MBS (5 ml) and 5% (w/v) sucrose in MBS (5 ml). The sucrose gradients were centrifuged at 33,000 rpm for 18 h at  $4^\circ\text{C}$  (Beckman SW40 rotor). 1-ml fractions were subsequently harvested from the top to the bottom of the tube. When necessary, protein fractions from the gradient were washed free of sucrose by dilution into 25 volumes of cold PBS and ultracentrifugation ( $150,000 \times g$ , for 1 h at  $4^\circ\text{C}$ ) to pellet the cholesterol-enriched microdomain material. Triton X-100-insoluble protein was resuspended in deglycosylation buffer and treated with PNGase-F as described.

**Basic pH Treatment of DRMs**—Triton X-100-insoluble membrane fractions were resuspended at  $4^\circ\text{C}$  in 0.1 M  $\text{K}_2\text{CO}_3$ , pH 11.5, or 0.1 M Tris, pH 7.4, incubated on ice for 20 min, and then centrifuged ( $150,000 \times g$  for 1 h at  $4^\circ\text{C}$ ) (21). The supernatants and pellets from both washes were separated, and the supernatants were concentrated by centrifugation through a 10-kDa cutoff filtration column (Amicon). Equal volumes of each fraction were analyzed by SDS-PAGE and immunoblotting.

**Immunocytochemistry on tsA-201 Cells**—The method used is essentially as described previously (22). Cells were fixed with 4% paraformaldehyde in TBS for 5 min at room temperature and then washed twice with TBS. Either no permeabilization step was used or cells were permeabilized for 15 min with 0.02% Triton X-100. The primary rat anti-HA (1:500) or mouse anti- $\alpha_2$ -1 (1:100) Abs were incubated overnight at  $4^\circ\text{C}$ , followed by Texas Red-conjugated anti-rabbit, Texas Red-conjugated anti-mouse, Alexa Fluor 488-conjugated anti-mouse (Molecular Probes) or biotinylated anti-rat Abs, and streptavidin-Alexa Fluor 488 (Invitrogen). All secondary antibodies were used in 1:500 dilution. 4',6-Diamidino-2-phenylindole (DAPI) was used to visualize the nuclei. Cells were mounted in Vectashield (Vector Laboratories, Burlingame, CA) to reduce photobleaching. Cells were examined on a confocal laser scanning microscope (Zeiss LSM), using a  $\times 40$  (1.3 NA) or  $\times 63$  (1.4 NA) oil-immersion objective. Confocal optical sections were  $1\ \mu\text{m}$ . Photomultiplier settings were kept constant in each experi-

ment, and all images were scanned sequentially. Image processing was performed using ImageJ. Data illustrated are representative of more than 10 cells each.

**Live Labeling of DRG Neuron Cultures**—DRG cultures were incubated with monoclonal rat anti-HA Ab (1:250, Roche Applied Science) for 1 h at  $37^\circ\text{C}$  in medium containing (in mM) the following: 145 NaCl; 5 KCl; 2  $\text{CaCl}_2$ ; 1  $\text{MgSO}_4$ ; 10 HEPES; 10 glucose, pH 7.4. Neurons were washed with PBS, fixed with 4% paraformaldehyde in PBS for 5 min and then blocked for 30–60 min with PBS supplemented with 10% goat serum. Secondary Ab (anti-rat Alexa Fluor 555, 1:500, Invitrogen) was applied for 2 h at room temperature. Samples were mounted and scanned as above.

**Electrophysiology**—Calcium channel currents were recorded in tsA-201 cells by whole cell patch-clamp recording, essentially as described previously (23). The internal (pipette) and external solutions and recording techniques were similar to those previously described (24). The patch pipette solution contained in mM: cesium aspartate, 140; EGTA, 5;  $\text{MgCl}_2$ , 2;  $\text{CaCl}_2$ , 0.1;  $\text{K}_2\text{ATP}$ , 2; HEPES, 10; pH 7.2, 310 mosM with sucrose. The external solution for recording  $\text{Ba}^{2+}$  currents contained in mM: tetraethylammonium bromide, 150; KCl, 3;  $\text{NaHCO}_3$ , 1.0;  $\text{MgCl}_2$ , 1.0; HEPES, 10; glucose, 4;  $\text{BaCl}_2$ , 1 or 5 as indicated, pH 7.4, 320 mosM with sucrose. Pipette of resistance 2–4 megohms were used. An Axopatch 1D amplifier (Axon Instruments, Burlingame, CA) was used, and data were filtered at 1–2 kHz and digitized at 5–10 kHz. Current records were subjected to leak and residual capacitance current subtraction (P/8 protocol). Analysis was performed using PCLAMP9 (Molecular Devices) and Origin 7 (Microcal Origin, Northampton, MA).

Current-voltage ( $I$ - $V$ ) plots were fit with a modified Boltzmann equation as described previously (25), for determination of the voltage for 50% activation ( $V_{50, \text{act}}$ ). Where data are given as mean  $\pm$  S.E., statistical comparisons were performed using either Student's  $t$  test or analysis of variance with post hoc test, as appropriate.

## RESULTS

**Expression of  $\alpha_2\delta$ -1 $\Delta$ C-term**—An anchorless  $\alpha_2\delta$ -1 construct ( $\alpha_2\delta$ -1 $\Delta$ C-term-HA) was made with a C-terminal HA tag (Fig. 1A, construct iii), to monitor expression. It was expressed in tsA-201 cells, and expression was compared with WT  $\alpha_2\delta$ -1 (Fig. 1A, construct i) and  $\alpha_2\delta$ -1 mid-HA (Fig. 1A, construct ii) in the WCL (Fig. 1B, lanes 2–4). The presence of a mid-HA tag in this position within  $\alpha_2$ -1 does not affect the function of the full-length  $\alpha_2\delta$ -1 (see Fig. 4A). Similar expression levels and a similar level of  $N$ -linked glycosylation, as shown by treatment with PNGase-F, were observed (Fig. 1B, top two panels,  $\alpha_2$ -1 Ab).

As found previously for heterologous expression of WT  $\alpha_2\delta$  subunits (15, 26), both  $\alpha_2\delta$ -1 mid-HA and  $\alpha_2\delta$ -1 $\Delta$ C-term-HA were only partially cleaved into  $\alpha_2$  and  $\delta$  (Fig. 1B, lanes 6–8). Partial cleavage is the reason that the  $\alpha_2$ -1 Ab recognizes two bands in reduced samples. These can best be distinguished following deglycosylation and have molecular masses of  $\sim 130$  kDa ( $\alpha_2\delta$ -1 “uncleaved form”) and  $\sim 105$  kDa ( $\alpha_2$ -1 “cleaved form”) (Fig. 1B, top right panel). As expected from the location of the HA epitope, in reduced deglycosylated samples, the HA

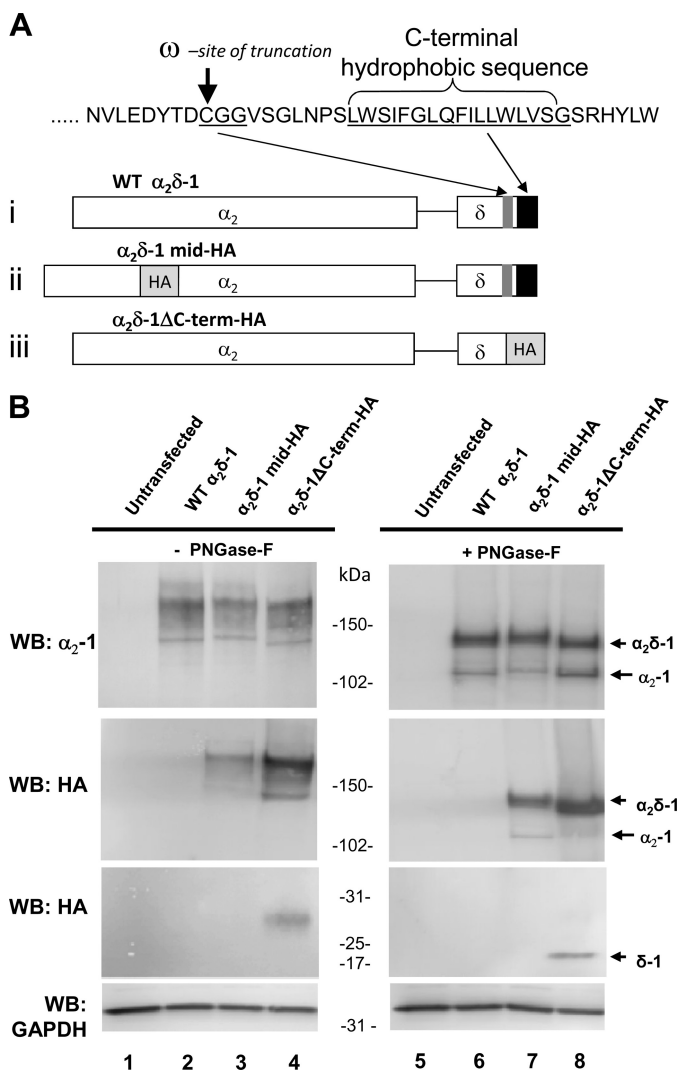


**FIGURE 1. Biochemical properties of  $\alpha_2\delta$ -1 $\Delta$ C-term-HA expressed in tsA-201 cells.** A, scheme of  $\alpha_2\delta$ -1 constructs used. The site of truncation and the position of the HA epitope (light gray box) are marked as follows: *construct i*, wild-type (WT)  $\alpha_2\delta$ -1; *construct ii*, full-length  $\alpha_2\delta$ -1 with an internal HA epitope ( $\alpha_2\delta$ -1 mid-HA); *construct iii*, truncated  $\alpha_2\delta$ -1 with C-terminal HA ( $\alpha_2\delta$ -1 $\Delta$ C-term-HA). The amino acid sequence of the C terminus of rat  $\alpha_2\delta$ -1, with the site of truncation at the GPI anchor attachment site predicted in our previous study (15) ( $\omega$ -site; C in CCGG underlined), and the C-terminal hydrophobic sequence (underlined) are shown at top. B, WCL from untransfected tsA-201 cells (lanes 1 and 5) or cells transfected with WT  $\alpha_2\delta$ -1 (lanes 2 and 6),  $\alpha_2\delta$ -1 mid-HA (lanes 3 and 7), or  $\alpha_2\delta$ -1 $\Delta$ C-term-HA (lanes 4 and 8), either untreated (left panel) or treated with PNGase-F (right panel). Bands were visualized with the indicated Abs, either against  $\alpha_2$ -1 (top panel) or against the HA epitope (middle two panels). The arrows on the right indicate bands corresponding to the deglycosylated proteins shown in the scheme in A, either uncleaved  $\alpha_2\delta$ -1 (upper band), cleaved  $\alpha_2$ -1 (lower band), or free  $\delta$ -1. The lower part of the same membrane was blotted with anti-GAPDH Ab as a loading control (bottom panel). WB, Western blot.

Ab revealed bands associated with uncleaved  $\alpha_2\delta$ -1 $\Delta$ C-term-HA (~130 kDa) and  $\delta$ -1 $\Delta$ C-term-HA peptide (~19 kDa) (Fig. 1B, lane 8). Note that the  $\alpha_2\delta$ -1 $\Delta$ C-term-HA showed increased HA immunoreactivity, compared with full-length  $\alpha_2\delta$ -1 mid-HA (Fig. 1B, middle panels). This is likely due to better accessibility of the C-terminally located HA epitope tag, rather than to increased expression levels of  $\alpha_2\delta$ -1 $\Delta$ C-term-HA, as the corresponding bands revealed by the  $\alpha_2$ -1 Ab were of similar intensities (Fig. 1B, top panel). To examine whether the

C-terminal HA tag was affecting the properties of the protein, we also made a truncated  $\alpha_2\delta$ -1 $\Delta$ C-term construct with an internal HA tag ( $\alpha_2\delta$ -1 mid-HA  $\Delta$ C-term) (supplemental Fig. 1A). This construct was similarly expressed (supplemental Fig. 1B) and glycosylated (data not shown), compared with  $\alpha_2\delta$ -1 mid-HA, and it was recognized by both  $\alpha_2$ -1 and HA Abs.

**Truncated  $\alpha_2\delta$ -1 $\Delta$ C-term Is Secreted into the Medium**—In medium conditioned by tsA-201 cells expressing  $\alpha_2\delta$ -1 $\Delta$ C-term-HA, we observed a band of ~165 kDa, which was immunoreactive to both  $\alpha_2$ -1 and HA Abs (Fig. 2A, lane 4), indicating that the anchorless construct was secreted. This band was absent from medium conditioned by untransfected cells or those expressing full-length WT  $\alpha_2\delta$ -1 or  $\alpha_2\delta$ -1 mid-HA (Fig. 2A, lanes 1–3).

The secreted anchorless protein was glycosylated, because PNGase-F treatment shifted the predominant band from ~165 to ~130 kDa, equivalent to the observed size of the unprocessed form of  $\alpha_2\delta$ -1 $\Delta$ C-term-HA after deglycosylation (Fig. 2B, lanes 1 and 2; see also Fig. 1B). Surprisingly, we barely detected any proteolytically processed  $\alpha_2\delta$ -1 $\Delta$ C-term in the medium, as demonstrated by the absence of  $\delta$ -1 $\Delta$ C-term-HA peptide in Fig. 2A (lane 4).

Transfection with increasing amounts of  $\alpha_2\delta$ -1 $\Delta$ C-term-HA cDNA (3, 6, or 10  $\mu$ g) resulted in increased expression and secretion of  $\alpha_2\delta$ -1 $\Delta$ C-term-HA at 72 h, as demonstrated by Western blot analysis (Fig. 2, C and D). We quantified the percentage of secreted  $\alpha_2\delta$ -1 $\Delta$ C-term-HA, relative to the total amount expressed, by measuring the mean intensity of bands and taking into account the total volume of each fraction, as described under “Experimental Procedures.” For this calculation, we have summed the cleaved and uncleaved  $\alpha_2\delta$ -1 bands detectable in WCL and in the media to obtain the total expression. The proportion of  $\alpha_2\delta$ -1 $\Delta$ C-term-HA secreted into the medium was  $75.6 \pm 2.8\%$  of the total amount of  $\alpha_2\delta$ -1 $\Delta$ C-term-HA expressed ( $n = 3$ ; Fig. 2E). Truncation within the hydrophobic domain resulting in a longer  $\alpha_2\delta$ -1 construct was previously shown to result in a construct that was partially secreted into the medium (27). The truncated construct with an internal HA tag ( $\alpha_2\delta$ -1 mid-HA  $\Delta$ C-term) also showed secretion into the medium as the uncleaved protein (supplemental Fig. 1C).

**Despite Removal of the Membrane Anchor,  $\alpha_2\delta$ -1 $\Delta$ C-term Remains in Part Associated with the Plasma Membrane**—We compared the distribution of full-length  $\alpha_2\delta$ -1 mid-HA to that of anchorless  $\alpha_2\delta$ -1 $\Delta$ C-term-HA, following heterologous expression in tsA-201 cells. Unexpectedly, we found that  $\alpha_2\delta$ -1 $\Delta$ C-term-HA was also associated with the plasma membrane in nonpermeabilized cells (Fig. 3A, panel ii), to a similar extent to the robust cell surface staining observed for  $\alpha_2\delta$ -1 mid-HA in nonpermeabilized cells (Fig. 3A, panel i) and to WT  $\alpha_2\delta$ -1, as demonstrated by anti- $\alpha_2$ -1 Ab staining (supplemental Fig. 2). In permeabilized cells, immunostaining was also observed intracellularly in both conditions (Fig. 3A, panels iii and iv). Association of  $\alpha_2\delta$ -1 $\Delta$ C-term-HA with the plasma membrane was not affected by co-transfection with an  $\alpha$ 1 and  $\beta$  subunit (Ca<sub>v</sub>2.2 and  $\beta$ 1b; Fig. 3B; supplemental Fig. 2, compare A and B), indicating that  $\alpha_2\delta$ -1 $\Delta$ C-term-HA does not require association with other calcium channel subunits for its membrane localiza-

## Anchorless $\alpha_2\delta$ -1 Enhances Calcium Currents

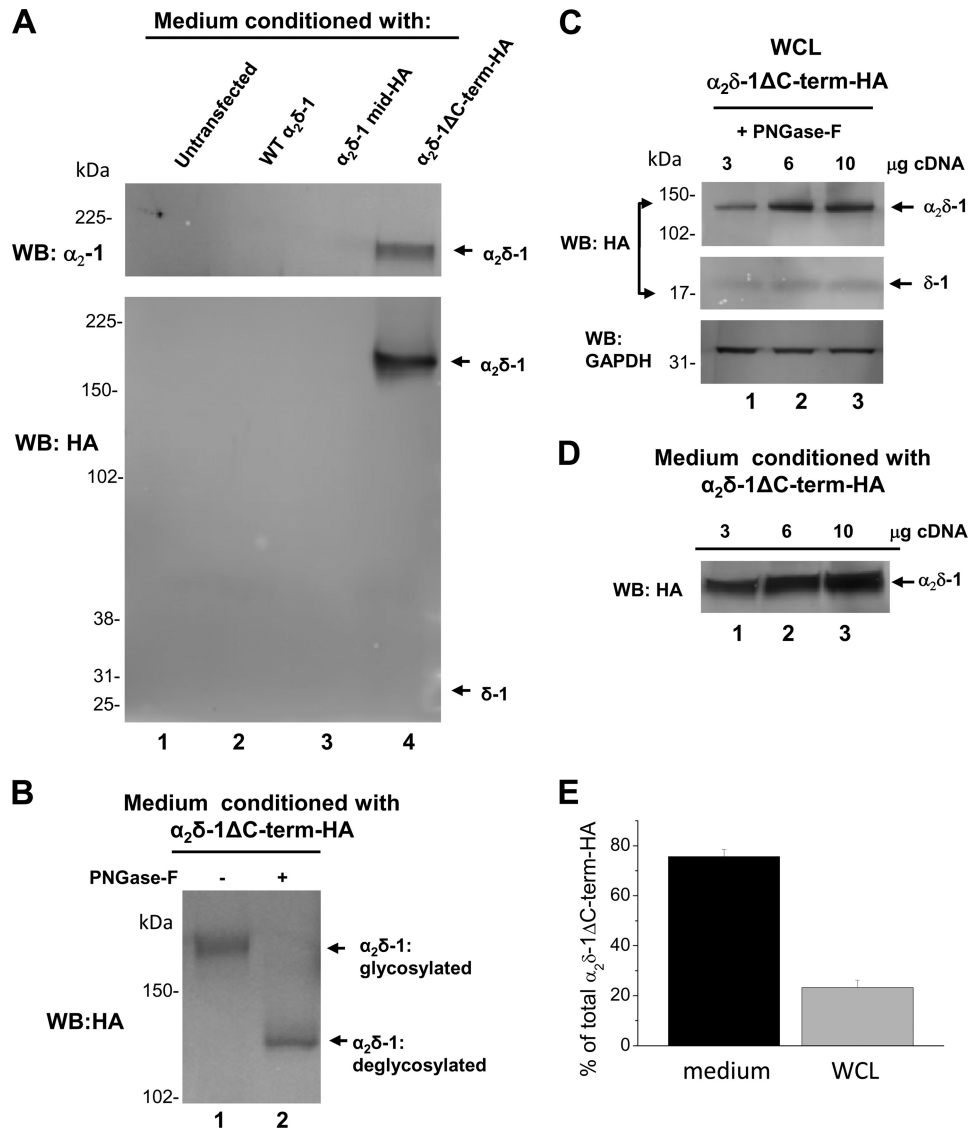


**FIGURE 2. Truncated  $\alpha_2\delta$ -1 $\Delta$ C-term-HA, but not full-length WT  $\alpha_2\delta$ -1 or  $\alpha_2\delta$ -1 mid-HA, is secreted into the medium as a glycosylated protein.** *A*, conditioned medium from untransfected tsA-201 cells (*lane 1*) or cells transfected with the full-length WT  $\alpha_2\delta$ -1 (*lane 2*),  $\alpha_2\delta$ -1 mid-HA (*lane 3*), or  $\alpha_2\delta$ -1 $\Delta$ C-term-HA (*lane 4*) was concentrated and analyzed as described under "Experimental Procedures." The Western blots (WB) were revealed with  $\alpha_2$ -1 Ab (*upper panel*) and HA Ab (*lower panel*). The arrows indicate a single band of  $\sim$ 165 kDa corresponding to the glycosylated uncleaved  $\alpha_2\delta$ -1 $\Delta$ C-term-HA, which was the main form found secreted in the medium. No secreted material was seen using WT  $\alpha_2\delta$ -1 or  $\alpha_2\delta$ -1 mid-HA-transfected cells (*lanes 2 and 3*) or untransfected cells (*lane 1*). *B*, conditioned medium, from cells transfected with  $\alpha_2\delta$ -1 $\Delta$ C-term-HA, was either untreated (*lane 1*) or treated with PNGase-F (*lane 2*). Bands were visualized with HA Ab. *C*, WCL from cells transfected with 3, 6, or 10  $\mu$ g of  $\alpha_2\delta$ -1 $\Delta$ C-term-HA cDNA was analyzed on blots visualized with anti-HA Ab. 20  $\mu$ g of total deglycosylated protein was loaded for each transfection condition. *D*, conditioned medium from the same cells was also blotted against HA Ab. An equal amount of medium was loaded for each condition. *E*, % of the total  $\alpha_2\delta$ -1 $\Delta$ C-term-HA that was either secreted (*black bar*) or present in the WCL (*gray bar*) was determined from three independent experiments ( $\pm$ S.E.), taking into account both the total volumes of the samples and the intensity of Western blot bands (see "Experimental Procedures"). Examples of gels used for this quantification are shown in *C* and *D*. Both the cleaved and uncleaved forms of  $\alpha_2\delta$ -1 $\Delta$ C-term-HA were included in this analysis.

tion. Furthermore, the fact that the HA epitope is exposed in nonpermeabilized  $\alpha_2\delta$ -1 $\Delta$ C-term-HA-transfected cells indicates that it has not utilized another hydrophobic region in the protein as a transmembrane domain, in which case the C-terminal HA tag would be intracellular. We also observed that, when expressed by nucleofection in DRG neurons,  $\alpha_2\delta$ -1 $\Delta$ C-term-HA was associated with the cell surface, both in the cell bodies and in neurites, to a similar extent to  $\alpha_2\delta$ -1 mid-HA (Fig. 3, *C* and *D*).

To rule out that the C-terminal HA tag was in some way artifactually mediating noncovalent membrane association, we also used the  $\alpha_2\delta$ -1 mid-HA  $\Delta$ C-term construct. We found that

this construct behaved similarly to  $\alpha_2\delta$ -1 $\Delta$ C-term-HA, being associated with the plasma membrane in nonpermeabilized cells (supplemental Fig. 1*D*), as well as being secreted (supplemental Fig. 1*C*).

*$\alpha_2\delta$ -1 $\Delta$ C-term-HA Retains Partial Functionality, in Terms of Enhancing Calcium Currents*—First, we showed that the full-length  $\alpha_2\delta$ -1 mid-HA construct used in this study retained full functionality in comparison with untagged full-length  $\alpha_2\delta$ -1 (WT  $\alpha_2\delta$ -1), in terms of increasing calcium currents relative to  $\text{Ca}_v2.1/\beta 1b$  alone (Fig. 4*A*). We then examined the ability of  $\alpha_2\delta$ -1 $\Delta$ C-term-HA to enhance  $\text{Ca}_v2.1/\beta 1b$  calcium currents, and surprisingly, we found that it retained substantial ability to

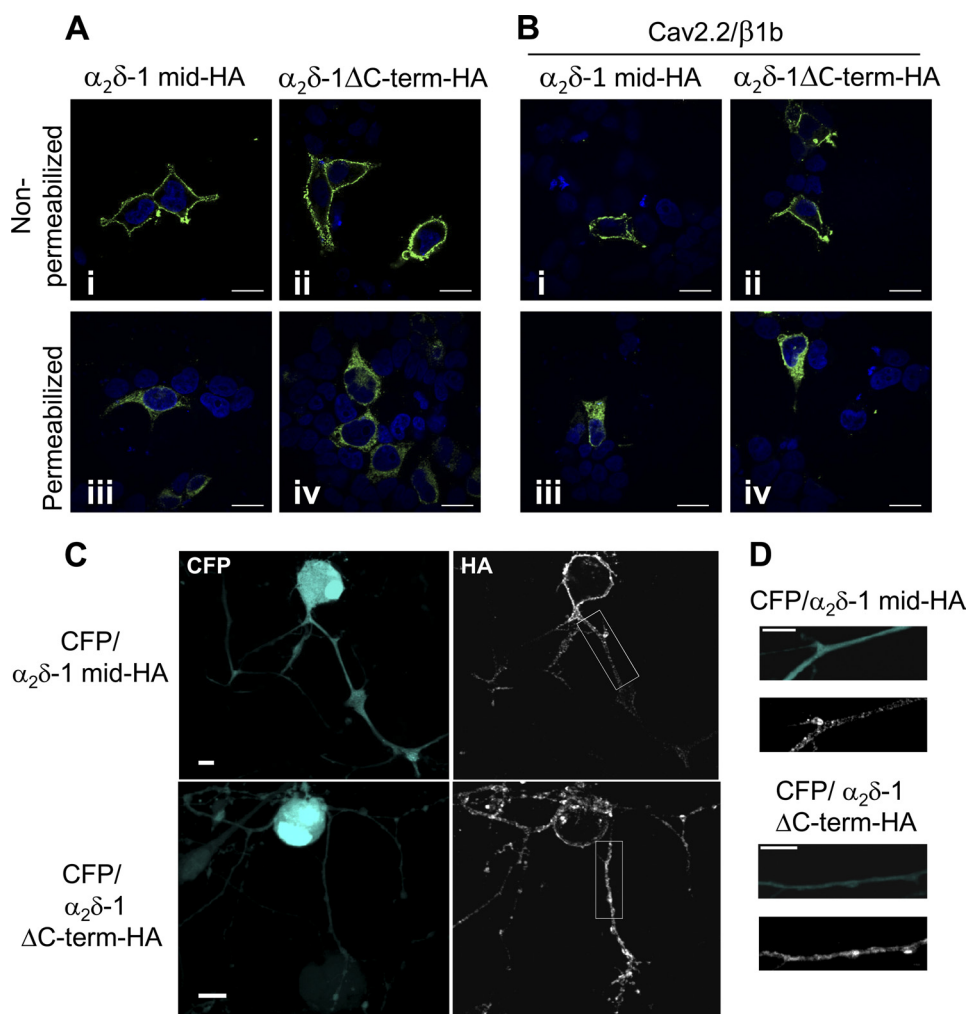


FIGURE 3. **A proportion of  $\alpha_2\delta$ -1 $\Delta$ C-term-HA is associated with the plasma membrane, independently of other  $\text{Ca}_v$  channel subunits.** *A*, confocal images of tsA-201 cells expressing either  $\alpha_2\delta$ -1 mid-HA (left, panels i and iii) or  $\alpha_2\delta$ -1 $\Delta$ C-term-HA (right, panels ii and iv). Immunostaining was performed using anti-HA Ab. Upper row, nonpermeabilized cells showing surface expression of both constructs. Lower row, cells were permeabilized with 0.02% Triton X-100 to show total expression. DAPI was used to visualize the nucleus (blue). *B*, confocal images of tsA-201 cells expressing  $\alpha_2\delta$ -1 mid-HA (left, panels i and iii) or  $\alpha_2\delta$ -1 $\Delta$ C-term-HA (right, panels ii and iv) both co-transfected with Cav2.2 and  $\beta$ 1b, stained with anti-HA Ab as in *A*. *C*, three-dimensional projection images of DRG neurons transfected with CFP/ $\alpha_2\delta$ -1 mid-HA or CFP/ $\alpha_2\delta$ -1 $\Delta$ C-term-HA. Cell surface detection of exogenous  $\alpha_2\delta$ -1 subunits was obtained by incubation of live neuronal cultures with anti-HA Ab (right) in CFP-positive neurons (left). Images are representative of nine CFP-positive neurons examined in each condition. *D*, higher magnification images of a neuronal process expressing CFP and labeled for surface  $\alpha_2\delta$ -1 mid-HA (upper panels) or  $\alpha_2\delta$ -1 $\Delta$ C-term-HA (lower panels). Scale bars, 20  $\mu\text{m}$  in *A* and *B* and 10  $\mu\text{m}$  in *C* and *D*.

cause an increase in these currents, relative to no  $\alpha_2\delta$  co-expression (Fig. 4, *B* and *C*), although the enhancement was smaller than that observed with WT  $\alpha_2\delta$ -1 (Fig. 4, *B* and *C*). In the absence of  $\alpha_2\delta$ -1, peak  $I_{\text{Ba}}$  at +5 mV (from Fig. 4*B*) was  $9.0 \pm 2.7\%$  of that in the presence of WT  $\alpha_2\delta$ -1, whereas for  $\alpha_2\delta$ -1 $\Delta$ C-term-HA it was  $38.5 \pm 7.6\%$ , representing a 3.8-fold increase over no  $\alpha_2\delta$  ( $p < 0.001$  compared with no  $\alpha_2\delta$ -1, analysis of variance, and Dunnett's post hoc test).

As observed previously (28), WT  $\alpha_2\delta$ -1 increased the inactivation rate of the peak  $\text{Ca}_v2.1/\beta$ 1b  $I_{\text{Ba}}$  (Fig. 4, *D* and *E*),  $\tau_{\text{inact}}$  being reduced from 177 ms in the absence of  $\alpha_2\delta$ -1 to 120 ms when WT  $\alpha_2\delta$ -1 was co-expressed. The truncated  $\alpha_2\delta$ -1 $\Delta$ C-term-HA had a less marked effect on inactivation, with  $\tau_{\text{inact}}$  being 145 ms (Fig. 4, *D* and *E*).

**Does Intercellular Transfer Occur from Secreted Anchorless  $\alpha_2\delta$ -1?**—To examine whether transcellular transfer of secreted  $\alpha_2\delta$ -1 $\Delta$ C-term-HA might occur via the medium to neighboring cells and contribute to plasma membrane association or cal-

cium current enhancement, tsA-201 cells expressing either  $\alpha_2\delta$ -1 mid-HA or  $\alpha_2\delta$ -1 $\Delta$ C-term-HA were co-cultured with cells expressing  $\text{Ca}_v2.1/\beta$ 1b/GFP. The cells were transfected separately and then washed and mixed after 5 h in culture. After a further 48 h in culture, cell surface  $\alpha_2\delta$ -1 was examined by immunocytochemistry in fixed nonpermeabilized cells, for both  $\alpha_2\delta$ -1 $\Delta$ C-term-HA and  $\alpha_2\delta$ -1 mid-HA (Fig. 5*A*, panels i and ii, red staining, white arrows), whereas GFP-positive cells were rarely found to be associated with any red staining. We found a very small amount of evidence of possible transfer of  $\alpha_2\delta$ -1 $\Delta$ C-term-HA to areas of the plasma membrane of  $\text{Ca}_v2.1/\beta$ 1b/GFP-transfected cells (indicated by a yellow arrow in Fig. 5*A*, panel i). No evidence of transfer of full-length  $\alpha_2\delta$ -1 mid-HA was observed (Fig. 5*A*, panel ii). These results suggest that attachment of  $\alpha_2\delta$ -1 $\Delta$ C-term-HA to cell surface components occurs mainly during the secretory process, rather than via secretion into the medium and reattachment.

## Anchorless $\alpha_2\delta$ -1 Enhances Calcium Currents

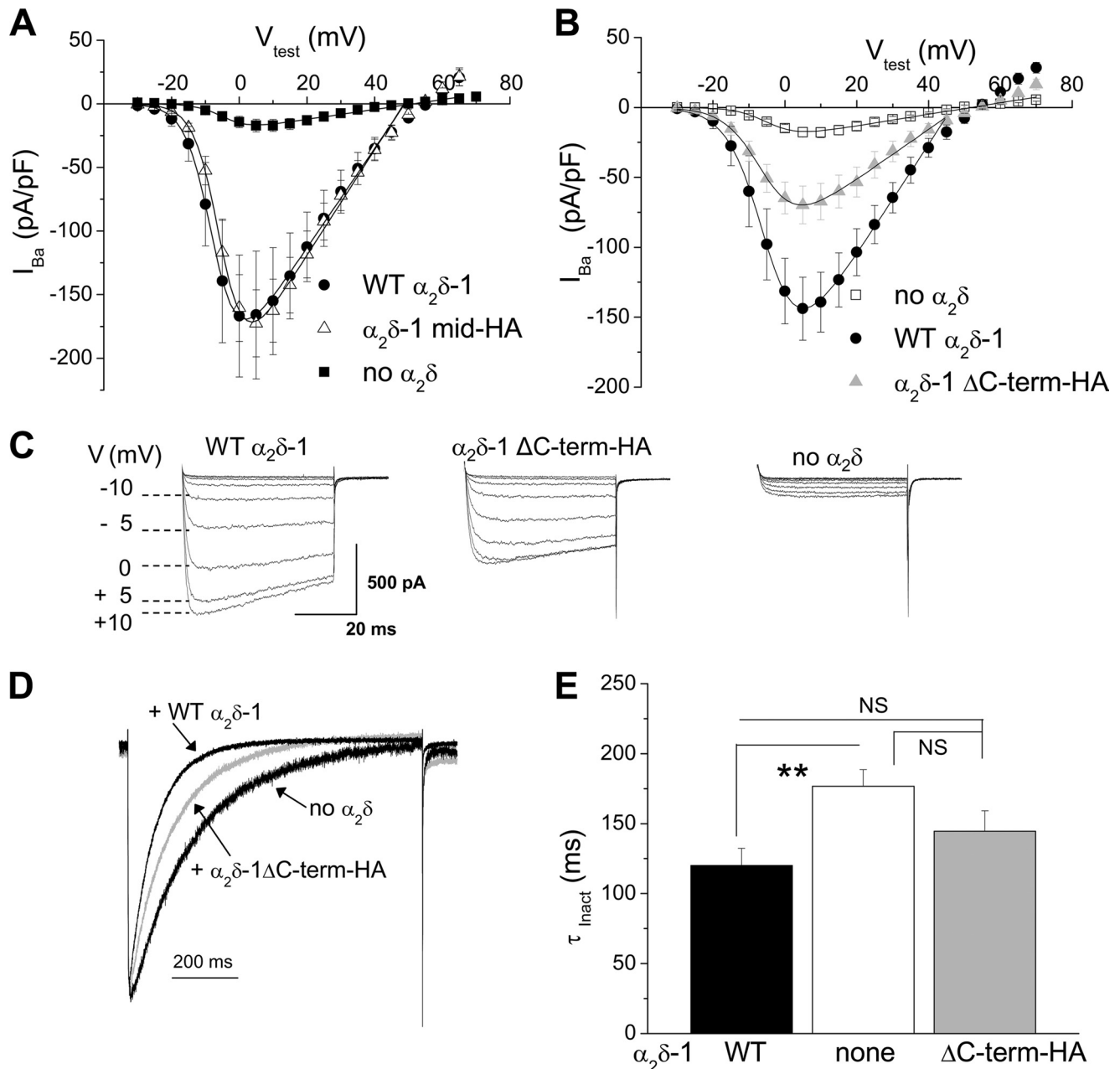


**FIGURE 4.  $\alpha_2\delta$ -1 $\Delta$ C-term-HA produces a partial enhancement of calcium channel currents.** *A*,  $I$ - $V$  relationships for  $Ca_v2.1$  plus  $\beta 1b$ , either alone (black squares,  $n = 6$ ) or co-expressing either WT  $\alpha_2\delta$ -1 (black circles,  $n = 6$ ) or  $\alpha_2\delta$ -1 mid-HA (white triangles,  $n = 7$ ). Data are mean  $\pm$  S.E. Data between  $-30$  and  $+50$  mV were fit with a modified Boltzmann function. The mean  $V_{50, act}$  values obtained were  $-4.2$ ,  $-7.3$ , and  $-5.3$  mV, respectively. *B*,  $I$ - $V$  relationships for  $Ca_v2.1$  plus  $\beta 1b$ , either alone (white squares,  $n = 8$ ) or co-expressing either WT  $\alpha_2\delta$ -1 (black circles,  $n = 8$ ) or  $\alpha_2\delta$ -1 $\Delta$ C-term-HA (gray triangles,  $n = 12$ ). Data are mean  $\pm$  S.E. Data between  $-30$  and  $+45$  mV were fit with a modified Boltzmann function. The  $V_{50, act}$  values obtained were  $-4.1$ ,  $-4.7$ , and  $-5.5$  mV, respectively. *C*, representative current traces for the three transfection conditions in response to depolarizing steps from  $-30$  to  $+10$  mV from  $V_H$  of  $-90$  mV as shown; calibration bars refer to all traces. *D*, representative  $I_{Ba}$  (normalized to the peak current), in response to 900 ms of depolarization to  $+5$  mV, to show differences in inactivation kinetics between  $Ca_v2.1/\beta 1b$  plus WT  $\alpha_2\delta$ -1 (rapidly inactivating black trace), without  $\alpha_2\delta$  (slowly inactivating black trace) and with  $\alpha_2\delta$ -1 $\Delta$ C-term-HA (gray trace). *E*, mean  $\tau_{inact}$  for  $I_{Ba}$  at  $+5$  mV for WT  $\alpha_2\delta$ -1 (black bar,  $n = 7$ ), in comparison with no  $\alpha_2\delta$  (white bar,  $n = 5$ ) and  $\alpha_2\delta$ -1 $\Delta$ C-term-HA (gray bar,  $n = 6$ ).  $I_{Ba}$  was recorded using  $1$  mM  $Ba^{2+}$ . Statistical differences were determined using one-way analysis of variance and Dunnett's post hoc test, where \*\*,  $p < 0.01$ , NS = nonsignificant.

Furthermore, co-culture of cells expressing  $Ca_v2.1/\beta 1b$  for 24–36 h directly with cells transfected with  $\alpha_2\delta$ -1 $\Delta$ C-term-HA, with  $\alpha_2\delta$ -1 mid-HA, or with empty vector as a control did not cause any increase in  $I_{Ba}$  recorded from these cells (Fig. 5B). Similarly, culture of tsA-201 cells expressing  $Ca_v2.1/\beta 1b$  for 5 h with medium conditioned by cells expressing  $\alpha_2\delta$ -1 $\Delta$ C-term-HA did not cause any increase in  $I_{Ba}$  compared with cells incubated with unconditioned medium (data not shown).

These results indicate that the enhancement of calcium currents only occurs after co-expression of  $\alpha_2\delta$ -1 $\Delta$ C-term-HA with the calcium channel  $\alpha_1$  and  $\beta$  subunits, and it is likely to involve an interaction of this construct with  $Ca_v2.1/\beta 1b$  channel complexes intracellularly, rather than once the  $\alpha_1/\beta$  complex has reached the plasma membrane.

*Anchorless  $\alpha_2\delta$ -1 $\Delta$ C-term-HA at the Plasma Membrane Is Proteolytically Processed to  $\alpha_2$  and  $\delta$  to a Greater Extent than*

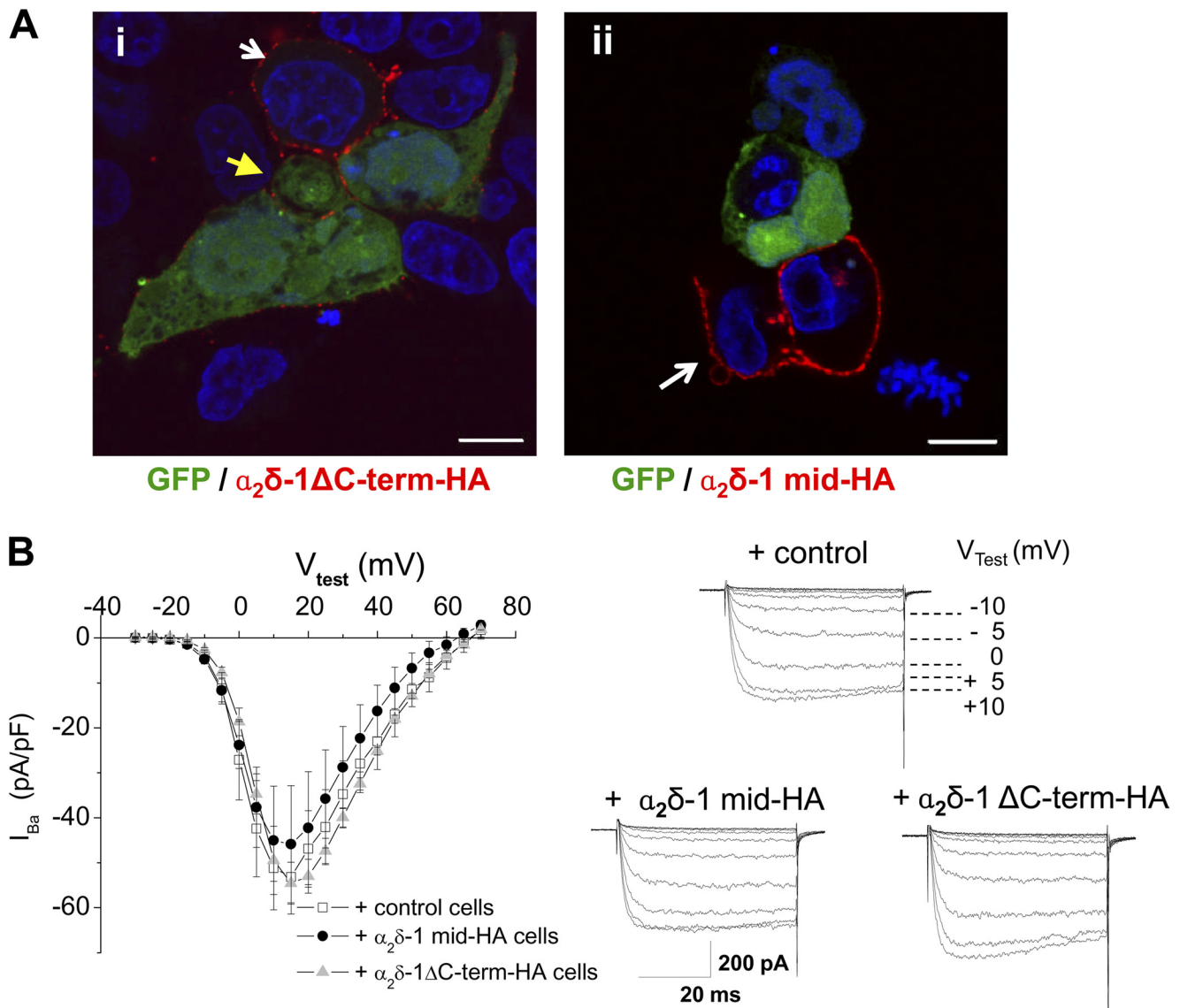


**FIGURE 5. Examination of whether intercellular transfer occurs for  $\alpha_2\delta$ -1 $\Delta$ C-term-HA.** *A*, images of cells expressing  $\text{Ca}_v2.1$  plus  $\beta 1b$  and GFP, mixed and co-cultured with cells expressing either  $\alpha_2\delta$ -1 $\Delta$ C-term-HA (left) or  $\alpha_2\delta$ -1 mid-HA (right). Cells were not permeabilized, and the HA tag is seen as red immunostaining, on cells transfected with  $\alpha_2\delta$ -1 $\Delta$ C-term-HA or WT  $\alpha_2\delta$ -1 mid-HA (white arrows). Cells expressing GFP were rarely found to have some small regions of red surface stain in the  $\alpha_2\delta$ -1 $\Delta$ C-term-HA condition (solid yellow arrow) but not in the  $\alpha_2\delta$ -1 mid-HA condition. DAPI was used to visualize cell nuclei (blue). Scale bars, 10  $\mu\text{m}$ . *B*, left, *I*-*V* relationship for cells expressing  $\text{Ca}_v2.1$  plus  $\beta 1b$  and GFP, co-cultured with cells expressing empty vector (white squares,  $n = 7$ ) or either  $\alpha_2\delta$ -1 mid-HA (black circles,  $n = 5$ ) or  $\alpha_2\delta$ -1 $\Delta$ C-term-HA (gray triangles,  $n = 7$ ). Data are mean  $\pm$  S.E. Right, representative current traces for each condition in response to depolarizing steps from  $-30$  to  $+10$  mV from  $V_H$  of  $-90$  mV as shown; calibration bars refer to all traces.  $I_{\text{Ba}}$  was recorded using 5 mM  $\text{Ba}^{2+}$  to record the small currents accurately.

*the Full-length  $\alpha_2\delta$ -1 mid-HA*—We next examined the properties of the  $\alpha_2\delta$ -1 $\Delta$ C-term-HA on the cell surface by cell surface biotinylation (Fig. 6A). Interestingly, we observed that  $\alpha_2\delta$ -1 $\Delta$ C-term-HA in the cell surface biotinylated fractions was proteolytically cleaved to form  $\alpha_2$ -1 to a greater extent, compared with the WCL (Fig. 6A, compare lanes 3 and 6). The proteolytic cleavage, quantified from three independent experiments, revealed an almost 2-fold increase of processing for  $\alpha_2\delta$ -1 $\Delta$ C-term-HA from the cell surface biotinylated fraction ( $80 \pm 4.7\%$  cleavage) compared with the corresponding WCL ( $43 \pm 6\%$ ) (Fig. 6B). In contrast, there was a smaller increase from  $38 \pm 4.5$  to  $50 \pm 3.3\%$ , respectively, for full-length  $\alpha_2\delta$ -1 mid-HA (Fig. 6). Therefore, the anchorless  $\alpha_2\delta$ -1 $\Delta$ C-term-HA that remained attached to the cell surface by an as yet unknown

mechanism was mainly processed to  $\alpha_2$ -1 and  $\delta$ . In contrast, the secreted form of  $\alpha_2\delta$ -1 $\Delta$ C-term-HA was predominantly unprocessed, as demonstrated by the absence of  $\delta$ -HA in the medium (Fig. 2A).

*Some  $\alpha_2\delta$ -1 $\Delta$ C-term Is Associated with Lipid Rafts*—Because some  $\alpha_2\delta$ -1 $\Delta$ C-term-HA was associated with the plasma membrane, we also examined whether it was still associated with DRMs, also termed lipid rafts, as demonstrated for WT  $\alpha_2\delta$ -1 and other  $\alpha_2\delta$  subunits (15, 26). We isolated DRMs from cells expressing WT  $\alpha_2\delta$ -1,  $\alpha_2\delta$ -1 mid-HA, or  $\alpha_2\delta$ -1 $\Delta$ C-term-HA by discontinuous sucrose gradient centrifugation as described previously (26). Untransfected tsA-201 cells express a small amount of endogenous  $\alpha_2\delta$ -1 (Fig. 7A), which localizes in DRMs. In transiently transfected tsA-201 cells,  $66 \pm 5.7\%$  of

## Anchorless $\alpha_2\delta$ -1 Enhances Calcium Currents

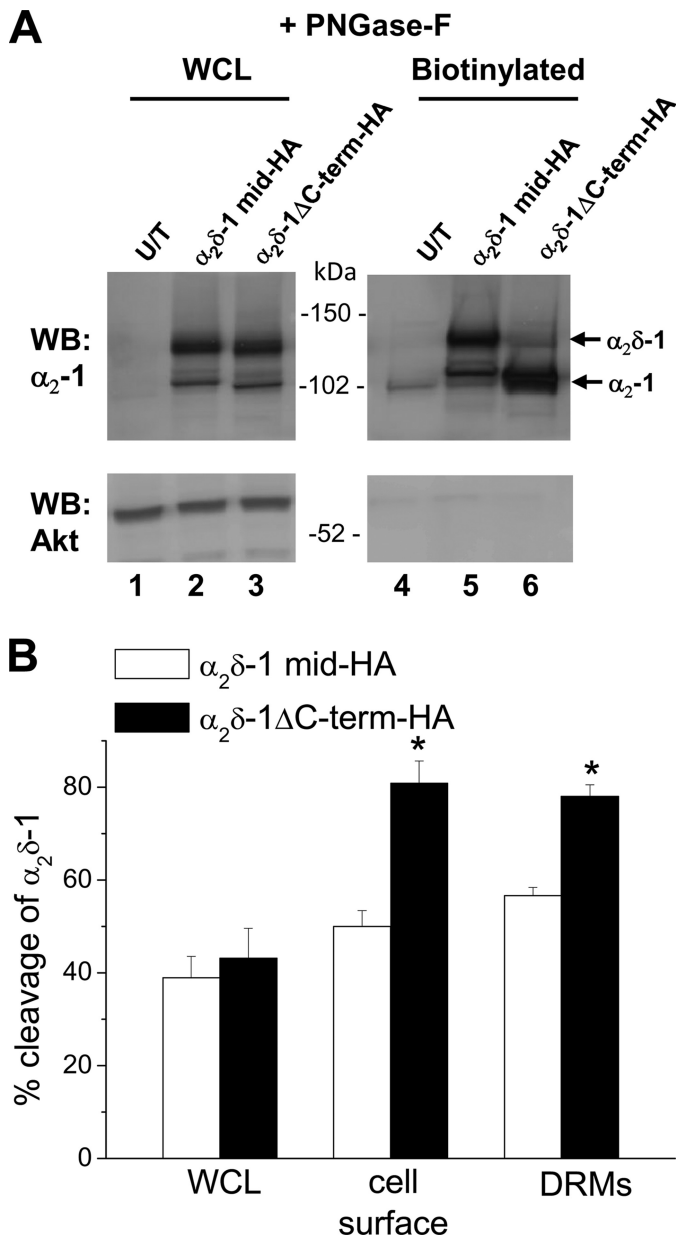


**FIGURE 6.  $\alpha_2\delta$ -1  $\Delta$ C-term-HA associated with the plasma membrane is highly processed to  $\alpha_2$ -1 and  $\delta$ -1.** *A*, samples of deglycosylated WCL (left panel) and precipitated cell surface-biotinylated proteins (right panel) from untransfected cells (UT, lanes 1 and 4) and cells transfected with  $\alpha_2\delta$ -1 mid-HA (lanes 2 and 5) or  $\alpha_2\delta$ -1 $\Delta$ C-term-HA (lanes 3 and 6) were resolved on a 3–8% Tris acetate gel. Western blots (WB) were revealed with  $\alpha_2$ -1 Ab. Lower panel, Western blotting with anti-Akt Ab (cytoplasmic protein) was used as a biotinylation control. Note the difference in relative proportions between the bands corresponding to  $\alpha_2\delta$ -1 and  $\alpha_2$ -1 in WCL (lanes 2 and 3) and cell surface biotinylated fractions (lanes 5 and 6). *B*, proteolytic cleavage of  $\alpha_2\delta$ -1 to  $\alpha_2$ -1 was calculated for different subcellular fractions for  $\alpha_2\delta$ -1 mid-HA (white bars) and  $\alpha_2\delta$ -1 $\Delta$ C-term-HA (black bars) using blots revealed with  $\alpha_2$ -1 Ab ( $n = 3$  independent experiments  $\pm$  S.E.); an example of one of the blots used for quantification of cleavage in the WCL and on the cell surface is shown in *A*, and for the DRM fraction is shown in Fig. 7, *E* and *F*. \*,  $p < 0.05$  compared with  $\alpha_2\delta$ -1 mid HA, Student's *t* test.

WT  $\alpha_2\delta$ -1 (Fig. 7B, fractions 5–7;  $n = 3$ ) and  $59.5 \pm 5.7\%$  of  $\alpha_2\delta$ -1 mid-HA (Fig. 7C,  $n = 3$ ) were found in DRM fractions. The DRM localization of the endogenous marker flotillin-1 was quantified to be  $85.4 \pm 3.9\%$ , whereas the transferrin receptor, which was used a marker for the soluble fractions, was essen-

tially absent from DRMs ( $n = 3$ ; Fig. 7, *A–D*). In contrast, we observed a large proportion of  $\alpha_2\delta$ -1 $\Delta$ C-term HA (Fig. 7D) and  $\alpha_2\delta$ -1 mid-HA  $\Delta$ C-term (supplemental Fig. 1) to be in the soluble fractions (11–13), as judged by both  $\alpha_2$ -1 and HA immunoreactivity. This distribution would be expected for a soluble protein in the process of being secreted. However, a significant fraction of both anchorless constructs ( $22.9 \pm 4.7\%$  of  $\alpha_2\delta$ -1 mid-HA  $\Delta$ C-term and  $29.1 \pm 2.1\%$  of  $\alpha_2\delta$ -1 $\Delta$ C-term-HA,  $n = 3$ ) remained associated with the DRMs (Fig. 7D and supplemental Fig. 1E). This result suggests that the GPI anchor is not the only means by which the protein is retained in DRMs.

As observed previously, proteolytic cleavage of  $\alpha_2\delta$ -1 to  $\alpha_2$  and  $\delta$  was more pronounced in isolated DRMs than in WCL (15, 26). However, that increase was greater for  $\alpha_2\delta$ -1 $\Delta$ C-term-HA (Fig. 7E) than for full-length  $\alpha_2\delta$ -1 mid-HA (Fig. 7F, quantification included in Fig. 6B). Therefore, similarly to the cell surface biotinylated  $\alpha_2\delta$ -1 $\Delta$ C-term-HA, isolated DRM fractions also contained more processed  $\alpha_2\delta$ -1 $\Delta$ C-term-HA (Fig. 6B).

*How Is  $\alpha_2\delta$ -1 $\Delta$ C-term Associated with the Plasma Membrane—* We examined a number of possibilities that could be responsible for the extrinsic interaction of  $\alpha_2\delta$ -1 $\Delta$ C-term with the cell surface. The fact that the HA epitope at the C terminus is accessible in nonpermeabilized cells strongly suggested that the truncated construct does not adopt a transmembrane configuration. To rule out the possibility that  $\alpha_2\delta$ -1 $\Delta$ C-term-HA formed an integral membrane protein, we treated DRMs isolated from cells expressing  $\alpha_2\delta$ -1 $\Delta$ C-term-HA or  $\alpha_2\delta$ -1 mid-HA with neutral (pH 7.4) or basic carbonate (pH 11.5) buffers. This method has been used previously to examine whether proteins are extrinsically associated with the membrane (16, 21, 29). We found that a high pH wash could release more  $\alpha_2\delta$ -1 $\Delta$ C-term-HA from DRMs into the supernatant, which was not the case for  $\alpha_2\delta$ -1 mid-HA. Less  $\alpha_2\delta$ -1 $\Delta$ C-term-HA was released by neutral pH washes (Fig. 8). This indicates that  $\alpha_2\delta$ -1 $\Delta$ C-term-HA is not an integral membrane protein, rather the interaction involves electrostatic association.

To test whether, similar to prion protein, the interaction of  $\alpha_2\delta$ -1 $\Delta$ C-term-HA with DRMs and cell surface involved interaction with glypicans, we treated cells with heparin (100  $\mu$ g/ml), which should interfere with any interaction with heparan sulfate proteoglycans. Incubation of either isolated DRMs or transfected cells with heparin had no effect on the association of  $\alpha_2\delta$ -1 $\Delta$ C-term-HA with DRMs or the plasma membrane (data not shown). We also found that mutation of the metal ion-dependent adhesion motif in the von Willebrand factor-A domain (6) of  $\alpha_2\delta$ -1 $\Delta$ C-term-HA did not prevent the protein from interacting with the plasma membrane (data not shown), indicating that the interaction does not require this site.

## DISCUSSION

The recent discovery that  $\alpha_2\delta$  subunits can be anchored to the membrane via a GPI moiety rather than a transmembrane protein domain has provided a novel point of view concerning some of their previously investigated properties as key modulators of  $Ca_v$  currents (10, 11). However, it has also opened new questions related to the role of membrane anchoring for the physiological function of  $\alpha_2\delta$  proteins. The initial aim of this

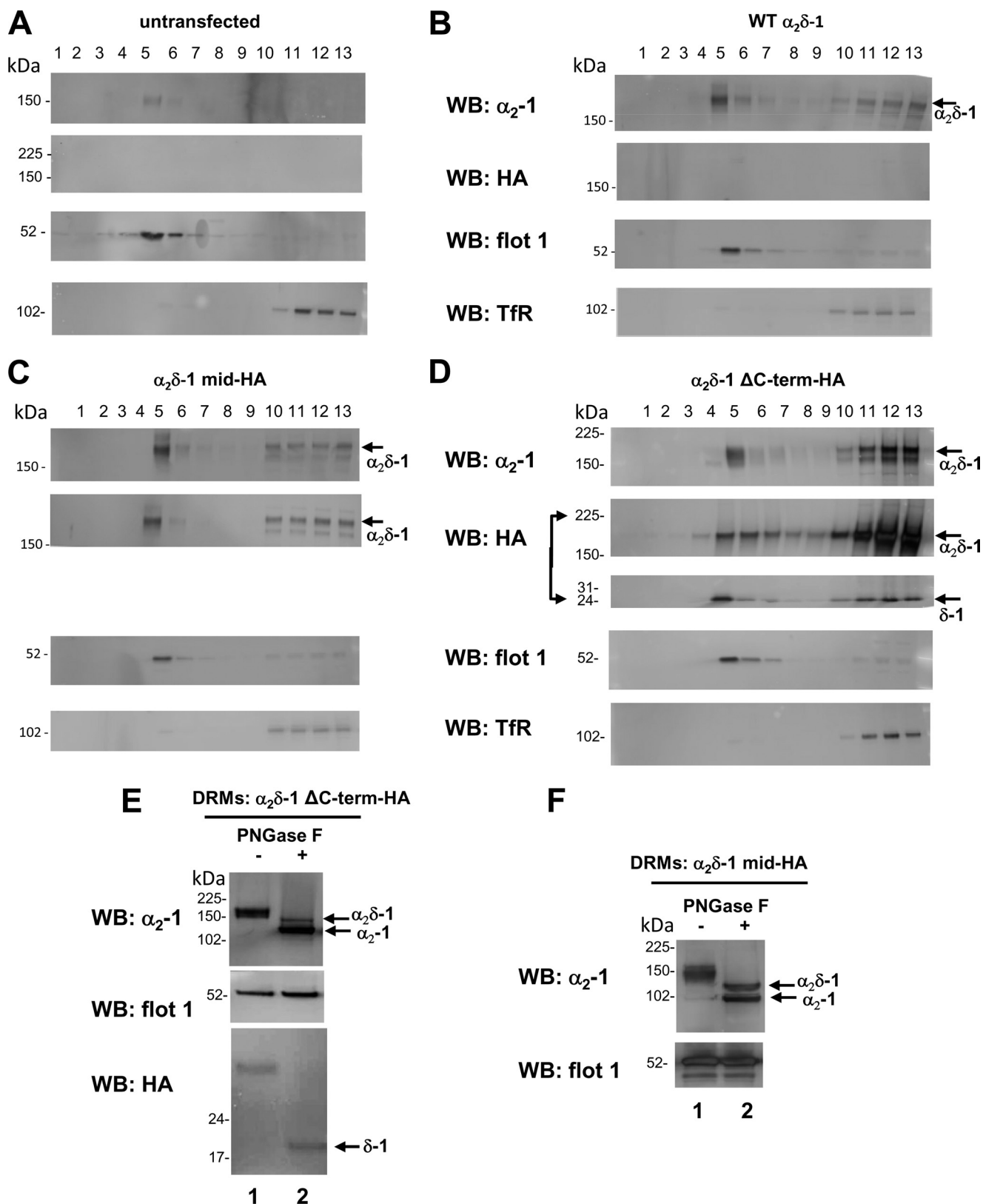
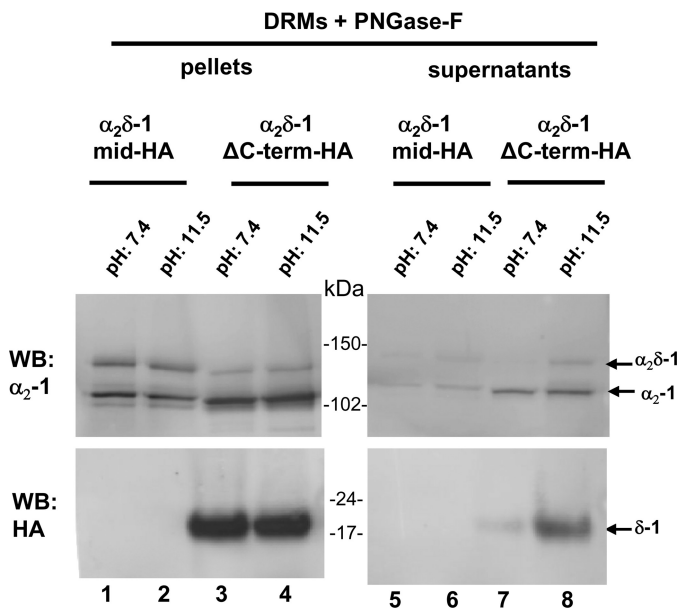


FIGURE 7.  $\alpha_2\delta$ -1 $\Delta$ C-term-HA is partially associated with DRMs. A–D, WCL from untransfected tsA-201 cells (A) or those expressing WT  $\alpha_2\delta$ -1 (B),  $\alpha_2\delta$ -1 mid-HA (C), or  $\alpha_2\delta$ -1 $\Delta$ C-term-HA (D) were subjected to sucrose gradient fractionation to isolate DRMs (fractions 5–7). Fractions were examined using  $\alpha_2$ -1 (top panels) and HA (middle panels) Abs. In each case, the distributions of the endogenous DRM marker, flotillin-1, and non-raft marker, transferrin receptor (TfR) were also examined (bottom two panels). Data are representative of at least three experiments. Quantification of % of material present in DRMs is given in the “Results.” E and F, isolated DRM fractions of  $\alpha_2\delta$ -1 $\Delta$ C-term-HA (E) and  $\alpha_2\delta$ -1 mid-HA (F)-transfected cells were deglycosylated with PNGase-F (lane 2 compared with lane 1) to show the presence of  $\alpha_2$ -1 (E and F) and  $\delta$ -1-HA (E). The % cleavage of  $\alpha_2\delta$ -1 into  $\alpha_2$ -1 and  $\delta$ -1 in DRMs is increased relative to WCL, as also shown in quantification on Fig. 6B.

## Anchorless $\alpha_2\delta$ -1 Enhances Calcium Currents



**FIGURE 8.  $\alpha_2\delta$ -1 $\Delta$ C-term-HA, but not  $\alpha_2\delta$ -1 mid-HA, is released from membranes by alkaline carbonate treatment.** Isolated DRM fractions from tsA-201 cells transfected with  $\alpha_2\delta$ -1 mid-HA (lanes 1, 2, 5, and 6) or  $\alpha_2\delta$ -1 $\Delta$ C-term-HA (lanes 3, 4, 7, and 8) were treated with buffer composed of either 0.1 M Tris, pH 7.4, or 0.1 M  $K_2CO_3$ , pH 11.5, as indicated, to dissociate extrinsically associated proteins. After centrifugation, the pellets (left panel) and supernatants (right panel) were deglycosylated with PNGase-F followed by Western blotting (top panel  $\alpha_2$ -1 Ab; bottom panel anti-HA Ab to reveal the  $\delta$ -1-HA peptide).

study was to address some of those issues with respect to membrane anchoring of  $\alpha_2\delta$ -1.

Previous *in vitro* studies have shown that  $\alpha_2\delta$ -1,  $\alpha_2\delta$ -2, and  $\alpha_2\delta$ -3 subunits all increase the maximum conductance of whole cell calcium channel currents arising from  $\alpha_1/\beta$  subunit combinations for the  $Ca_v1$  and  $Ca_v2$  classes, in several different expression systems (30–34). For  $\alpha_2\delta$ -1, it was previously shown that expression of the  $\alpha_2$ -1 or  $\delta$ -1 alone did not enhance calcium currents through  $Ca_v2.1$  channels (10). Furthermore, these authors also found that expression of  $\alpha_2\delta$ -1 with the transmembrane segment from another protein (adhelin) did not enhance calcium currents, which is now unsurprising in the light of our recent finding that the  $\alpha_2\delta$  subunits can form GPI-anchored proteins (15). Replacing the transmembrane segment with an unrelated sequence might interfere with the cleavage of GPI-anchoring signal sequence and the subsequent attachment of the GPI moiety. It has been found that uncleaved GPI precursor proteins show aggregation in the endoplasmic reticulum (35).

It was initially suggested that the transmembrane segment of  $\delta$  was required for calcium current stimulation, and the entire extracellular portion of  $\alpha_2\delta$ -1 was implicated in subunit interaction with  $Ca_v2.1$  (10). Moreover, co-expression of  $Ca_v2.1$  channels with  $\delta$ -1 alone affected the biophysical properties of the currents but did not enhance their amplitudes (26). We have now revisited this issue with respect to our recent findings that  $\alpha_2\delta$  subunits can form GPI-anchored proteins.

We have created an anchorless  $\alpha_2\delta$ -1 ( $\alpha_2\delta$ -1 $\Delta$ C-term) by adding a stop codon immediately prior to the predicted site of attachment of the GPI moiety (15, 36). This approach has previously been employed successfully to study the role of GPI

anchoring on the behavior of the prion protein (16). By this means, we obtained a soluble protein deprived of hydrophobic membrane anchoring but containing  $\alpha_2$ -1 and all the extracellular parts of  $\delta$ -1, both of which were both previously shown to be of major importance for channel regulation and interaction (11, 26). In our study we found the surprising result that the C-terminal membrane anchoring is not the only determinant of the ability of  $\alpha_2\delta$ -1 to enhance calcium channel currents, because  $\alpha_2\delta$ -1 $\Delta$ C-term still produced a substantial increase of calcium currents when co-expressed with  $Ca_v2.1$  and  $\beta 1b$ . Interestingly, we did not observe such effects upon external application of secreted  $\alpha_2\delta$ -1 $\Delta$ C-term to cells previously transfected with  $Ca_v2.1$  and  $\beta 1b$ , suggesting that an intracellular interaction with other subunits is required for the functionality of  $\alpha_2\delta$ -1 in the calcium channel complex. Moreover, this result implies that other factors than membrane anchoring are likely to be involved in the current-potentiating effects of  $\alpha_2\delta$ -1.

As expected, a large proportion of  $\alpha_2\delta$ -1 $\Delta$ C-term is secreted into the medium, when it is expressed in tsA-201 cells. However, we also found, using both immunocytochemistry and cell surface biotinylation, that  $\alpha_2\delta$ -1 $\Delta$ C-term constructs, despite the lack of a C-terminal membrane anchor, remain partially associated with the plasma membrane. However,  $\alpha_2\delta$ -1 $\Delta$ C-term-HA does not utilize another hydrophobic region as a transmembrane anchor, because both the  $\alpha_2$ -1 and HA Abs can access their epitopes in nonpermeabilized cells.

The interaction of  $\alpha_2\delta$ -1 $\Delta$ C-term with membranes occurs via a noncovalent linkage, because alkaline carbonate treatment disrupted the DRM association. Furthermore, the interaction is not affected by the presence or absence of other calcium channel subunits. Our finding that secreted  $\alpha_2\delta$ -1 $\Delta$ C-term does not re-attach to the plasma membrane following secretion further suggests that its association with the plasma membrane occurs during the maturation and trafficking of the protein.

There are 16 predicted N-linked glycosylation sites in the rat  $\alpha_2\delta$ -1 sequence. We have found that secreted  $\alpha_2\delta$ -1 $\Delta$ C-term was heavily glycosylated, because PNGase-F removed all N-glycosylation (~35 kDa) producing a shift to an apparent mass of ~130 kDa, corresponding to unprocessed deglycosylated  $\alpha_2\delta$ -1 $\Delta$ C-term (Fig. 2B).

We have shown in our previous studies that  $\alpha_2\delta$  subunits are strongly localized in DRMs, both in native tissue and following heterologous expression (15, 26). The GPI-anchoring of  $\alpha_2\delta$  subunits, as for other proteins, is likely to be an important determinant of their localization in these domains (15) but not the sole factor (16, 37). This is reinforced by the finding that  $\alpha_2\delta$ -1 $\Delta$ C-term remains, in part, associated with DRMs. Much of the DRM fraction is derived from the cholesterol-rich plasma membrane, as determined by combined cell surface biotinylation and DRM studies (17). Thus, the partial association of the  $\alpha_2\delta$ -1 $\Delta$ C-term constructs with DRMs is in agreement with our evidence that some  $\alpha_2\delta$ -1 $\Delta$ C-term is associated with the plasma membrane.

Removal of the C-terminal GPI anchor signal sequence from prion protein did not completely prevent its lipid raft or membrane association (16), although the anchorless prion protein was mainly secreted. Furthermore, prion protein was found to interact with GPI-anchored heparan sulfate proteoglycans

(glypicans), which play a role in retaining it in DRM fractions (17). In contrast, in this study heparin, which should disrupt such an interaction, did not prevent cell surface or DRM association of  $\alpha_2\delta$ -1 $\Delta$ C-term.

We have found previously that heterologously expressed  $\alpha_2\delta$  proteins are only partially proteolytically processed into  $\alpha_2$  and  $\delta$  in many expression systems (15, 26, 38). This behavior of expressed  $\alpha_2\delta$  subunits contrasts with the complete processing of native  $\alpha_2\delta$  proteins, where no full-length  $\alpha_2\delta$  is observed (15, 38). In this study, we found that  $\alpha_2\delta$ -1 $\Delta$ C-term is also incompletely processed, and in particular the secreted form shows very little proteolytic cleavage. In contrast,  $\alpha_2\delta$ -1 $\Delta$ C-term in both the DRM fraction and the cell surface-biotinylated fraction exhibits a much greater proportion of cleaved  $\alpha_2$ -1 and  $\delta$ -1 $\Delta$ C-term than the WCL or the secreted fraction. These results indicate that the protease in question is likely to be absent from the constitutive secretory pathway, but it is present in the biogenesis pathway for membrane components. The increased proteolytic cleavage of plasma membrane and DRM-associated  $\alpha_2\delta$ -1 $\Delta$ C-term, compared with full-length  $\alpha_2\delta$ -1, may result from its greater flexibility and availability as a substrate. Furthermore, a number of proteases have also been localized to lipid rafts (39, 40), which may relate to the increased processing of  $\alpha_2\delta$  in DRM fractions.

Because it has been found that the proteolytic cleavage of  $\alpha_2\delta$ -1 is important for its function to enhance calcium channel currents (41), it is likely that the proteolytically cleaved  $\alpha_2\delta$ -1 $\Delta$ C-term associated with the plasma membrane is responsible for its function, but this remains to be conclusively demonstrated by using a protease-deficient mutant of  $\alpha_2\delta$ -1 $\Delta$ C-term.

The main physiological relevance of this study is that the truncation of  $\alpha_2\delta$ -1 at its predicted GPI anchor site does not prevent the ability of this construct to affect calcium channel function. This indicates that intrinsic association of  $\alpha_2\delta$ -1 to the plasma membrane is not essential for its function. Our finding that anchorless  $\alpha_2\delta$ -1 is still in part extrinsically associated with the plasma membrane and DRMs suggests that  $\alpha_2\delta$ -1 $\Delta$ C-term may be processed by two alternative routes, a secretory pathway and a membrane biogenesis pathway, and in the latter pathway it becomes associated with one or more binding partners that determine its association with membranes. This now gives us an important means of identifying the physiological binding partner(s) of  $\alpha_2\delta$  proteins involved in controlling their trafficking and cell surface localization.

Our future research will therefore be aimed at identifying the binding partner(s) with which  $\alpha_2\delta$ -1 $\Delta$ C-term is interacting during the trafficking process, and which may also serve to tether it to the plasma membrane. It will also be of great interest to determine whether this interaction is related to the surprising ability of  $\alpha_2\delta$ -1 $\Delta$ C-term to produce a partial enhancement of calcium channel currents.

## REFERENCES

- Catterall, W. A. (2000) Structure and regulation of voltage-gated  $\text{Ca}^{2+}$  channels. *Annu. Rev. Cell Dev. Biol.* **16**, 521–555
- Dolphin, A. C. (2003)  $\beta$  subunits of voltage-gated calcium channels. *J. Bioenerg. Biomembr.* **35**, 599–620
- Leroy, J., Richards, M. W., Richards, M. S., Butcher, A. J., Nieto-Rostro, M., Pratt, W. S., Davies, A., and Dolphin, A. C. (2005) Interaction via a key tryptophan in the I-II linker of *N*-type calcium channels is required for  $\beta 1$  but not for palmitoylated  $\beta 2$ , implicating an additional binding site in the regulation of channel voltage-dependent properties. *J. Neurosci.* **25**, 6984–6996
- Waithe, D., Ferron, L., Page, K. M., Chaggar, K., and Dolphin, A. C. (2011)  $\beta$ -Subunits promote the expression of  $\text{Ca}_v2.2$  channels by reducing their proteasomal degradation. *J. Biol. Chem.* **286**, 9598–9611
- Canti, C., Davies, A., and Dolphin, A. C. (2003) Calcium channel  $\alpha_2\delta$  subunits: structure, functions and target site for drugs. *Curr. Neuropharmacol.* **1**, 209–217
- Canti, C., Nieto-Rostro, M., Foucault, I., Heblich, F., Wratten, J., Richards, M. W., Hendrich, J., Douglas, L., Page, K. M., Davies, A., and Dolphin, A. C. (2005) The metal ion-dependent adhesion site in the von Willebrand factor-A domain of  $\alpha_2\delta$  subunits is key to trafficking voltage-gated  $\text{Ca}^{2+}$  channels. *Proc. Natl. Acad. Sci. U.S.A.* **102**, 11230–11235
- Davies, A., Hendrich, J., Van Minh, A. T., Wratten, J., Douglas, L., and Dolphin, A. C. (2007) Functional biology of the  $\alpha_2\delta$  subunits of voltage-gated calcium channels. *Trends Pharmacol. Sci.* **28**, 220–228
- Ertel, E. A., Campbell, K. P., Harpold, M. M., Hofmann, F., Mori, Y., Perez-Reyes, E., Schwartz, A., Snutch, T. P., Tanabe, T., Birnbaumer, L., Tsien, R. W., and Catterall, W. A. (2000) Nomenclature of voltage-gated calcium channels. *Neuron* **25**, 533–535
- Burgess, D. L., Gefrides, L. A., Foreman, P. J., and Noebels, J. L. (2001) A cluster of three novel  $\text{Ca}^{2+}$  channel  $\gamma$  subunit genes on chromosome 19q13.4. Evolution and expression profile of the  $\gamma$  subunit gene family. *Genomics* **71**, 339–350
- Gurnett, C. A., De Waard, M., and Campbell, K. P. (1996) Dual function of the voltage-dependent  $\text{Ca}^{2+}$  channel  $\alpha_2\delta$  subunit in current stimulation and subunit interaction. *Neuron* **16**, 431–440
- Gurnett, C. A., Felix, R., and Campbell, K. P. (1997) Extracellular interaction of the voltage-dependent  $\text{Ca}^{2+}$  channel  $\alpha_2\delta$  and  $\alpha 1$  subunits. *J. Biol. Chem.* **272**, 18508–18512
- Ellis, S. B., Williams, M. E., Ways, N. R., Brenner, R., Sharp, A. H., Leung, A. T., Campbell, K. P., McKenna, E., Koch, W. J., and Hui, A. (1988) Sequence and expression of mRNAs encoding the  $\alpha 1$  and  $\alpha 2$  subunits of a DHP-sensitive calcium channel. *Science* **241**, 1661–1664
- Jay, S. D., Sharp, A. H., Kahl, S. D., Vedvick, T. S., Harpold, M. M., and Campbell, K. P. (1991) Structural characterization of the dihydropyridine-sensitive calcium channel  $\alpha 2$ -subunit and the associated  $\delta$  peptides. *J. Biol. Chem.* **266**, 3287–3293
- Hoppa, M. B., Lana, B., Margas, W., Dolphin, A. C., and Ryan, T. A. (2012)  $\alpha_2\delta$  expression sets presynaptic calcium channel abundance and release probability. *Nature* **486**, 122–125
- Davies, A., Kadurin, I., Alvarez-Laviada, A., Douglas, L., Nieto-Rostro, M., Bauer, C. S., Pratt, W. S., and Dolphin, A. C. (2010) The  $\alpha_2\delta$  subunits of voltage-gated calcium channels form GPI-anchored proteins, a posttranslational modification essential for function. *Proc. Natl. Acad. Sci. U.S.A.* **107**, 1654–1659
- Campana, V., Caputo, A., Sarnataro, D., Paladino, S., Tivodar, S., and Zurzolo, C. (2007) Characterization of the properties and trafficking of an anchorless form of the prion protein. *J. Biol. Chem.* **282**, 22747–22756
- Taylor, D. R., Whitehouse, I. J., and Hooper, N. M. (2009) Glypican-1 mediates both prion protein lipid raft association and disease isoform formation. *PLoS Pathog.* **5**, e1000666
- Tomlinson, W. J., Stea, A., Bourinet, E., Charnet, P., Nargeot, J., and Snutch, T. P. (1993) Functional properties of a neuronal class C L-type calcium channel. *Neuropharmacology* **32**, 1117–1126
- Cormack, B. P., Valdivia, R. H., and Falkow, S. (1996) FACS-optimized mutants of the green fluorescent protein (GFP). *Gene* **173**, 33–38
- Page, K. M., Heblich, F., Davies, A., Butcher, A. J., Leroy, J., Bertaso, F., Pratt, W. S., and Dolphin, A. C. (2004) Dominant-negative calcium channel suppression by truncated constructs involves a kinase implicated in the unfolded protein response. *J. Neurosci.* **24**, 5400–5409
- Fujiki, Y., Hubbard, A. L., Fowler, S., and Lazarow, P. B. (1982) Isolation of intracellular membranes by means of sodium carbonate treatment. Application to endoplasmic reticulum. *J. Cell Biol.* **93**, 97–102
- Brice, N. L., Berrow, N. S., Campbell, V., Page, K. M., Brickley, K., Tedder, L., and Dolphin, A. C. (1997) Importance of the different  $\beta$  subunits in the

## Anchorless $\alpha_2\delta$ -1 Enhances Calcium Currents

- membrane expression of the  $\alpha$ 1A and  $\alpha$ 2 calcium channel subunits. Studies using a depolarization-sensitive  $\alpha$ 1A antibody. *Eur. J. Neurosci.* **9**, 749–759
23. Berrow, N. S., Brice, N. L., Tedder, I., Page, K. M., and Dolphin, A. C. (1997) Properties of cloned rat  $\alpha$ 1A calcium channels transiently expressed in the COS-7 cell line. *Eur. J. Neurosci.* **9**, 739–748
  24. Campbell, V., Berrow, N. S., Fitzgerald, E. M., Brickley, K., and Dolphin, A. C. (1995) Inhibition of the interaction of G protein  $G_o$  with calcium channels by the calcium channel  $\beta$ -subunit in rat neurones. *J. Physiol.* **485**, 365–372
  25. Cantì, C., Davies, A., Berrow, N. S., Butcher, A. J., Page, K. M., and Dolphin, A. C. (2001) Evidence for two concentration-dependent processes for  $\beta$ -subunit effects on  $\alpha$ 1B calcium channels. *Biophys. J.* **81**, 1439–1451
  26. Davies, A., Douglas, L., Hendrich, J., Wratten, J., Tran Van Minh, A., Foucault, I., Koch, D., Pratt, W. S., Saibil, H. R., and Dolphin, A. C. (2006) The calcium channel  $\alpha_2\delta$  2 subunit partitions with CaV2.1 into lipid rafts in cerebellum. Implications for localization and function. *J. Neurosci.* **26**, 8748–8757
  27. Brown, J. P., and Gee, N. S. (1998) Cloning and deletion mutagenesis of the  $\alpha_2\delta$  calcium channel subunit from porcine cerebral cortex. Expression of a soluble form of the protein that retains [ $^3$ H]gabapentin binding activity. *J. Biol. Chem.* **273**, 25458–25465
  28. Felix, R., Gurnett, C. A., De Waard, M., and Campbell, K. P. (1997) Dissection of functional domains of the voltage-dependent  $Ca^{2+}$  channel  $\alpha_2\delta$  subunit. *J. Neurosci.* **17**, 6884–6891
  29. Brown, D. A., and Rose, J. K. (1992) Sorting of GPI-anchored proteins to glycolipid-enriched membrane subdomains during transport to the apical cell surface. *Cell* **68**, 533–544
  30. Walker, D., and De Waard, M. (1998) Subunit interaction sites in voltage-dependent  $Ca^{2+}$  channels. Role in channel function. *Trends Neurosci.* **21**, 148–154
  31. Mori, Y., Friedrich, T., Kim, M. S., Mikami, A., Nakai, J., Ruth, P., Bosse, E., Hofmann, F., Flockerzi, V., and Furuichi, T. (1991) Primary structure and functional expression from complementary DNA of a brain calcium channel. *Nature* **350**, 398–402
  32. Klugbauer, N., Lacinová, L., Marais, E., Hobom, M., and Hofmann, F. (1999) Molecular diversity of the calcium channel  $\alpha_2\delta$  subunit. *J. Neurosci.* **19**, 684–691
  33. Dolphin, A. C., Wyatt, C. N., Richards, J., Beattie, R. E., Craig, P., Lee, J. H., Cribbs, L. L., Volsen, S. G., and Perez-Reyes, E. (1999) The effect of  $\alpha_2\delta$  and other accessory subunits on expression and properties of the calcium channel  $\alpha$ 1G. *J. Physiol.* **519**, 35–45
  34. Hobom, M., Dai, S., Marais, E., Lacinova, L., Hofmann, F., and Klugbauer, N. (2000) Neuronal distribution and functional characterization of the calcium channel  $\alpha_2\delta$ -2 subunit. *Eur. J. Neurosci.* **12**, 1217–1226
  35. Delahunty, M. D., Stafford, F. J., Yuan, L. C., Shaz, D., and Bonifacino, J. S. (1993) Uncleaved signals for glycosylphosphatidylinositol anchoring cause retention of precursor proteins in the endoplasmic reticulum. *J. Biol. Chem.* **268**, 12017–12027
  36. Pierleoni, A., Martelli, P. L., and Casadio, R. (2008) PredGPI. A GPI-anchor predictor. *BMC Bioinformatics* **9**, 392
  37. Robinson, P., Etheridge, S., Song, L., Shah, R., Fitzgerald, E. M., and Jones, O. T. (2011) Targeting of voltage-gated calcium channel  $\alpha_2\delta$ -1 subunit to lipid rafts is independent from a GPI-anchoring motif. *PLoS ONE* **6**, e19802
  38. Douglas, L., Davies, A., Wratten, J., and Dolphin, A. C. (2006) Do voltage-gated calcium channel  $\alpha_2\delta$  subunits require proteolytic processing into  $\alpha_2$  and  $\delta$  to be functional? *Biochem. Soc. Trans.* **34**, 894–898
  39. Cordy, J. M., Hussain, I., Dingwall, C., Hooper, N. M., and Turner, A. J. (2003) Exclusively targeting  $\beta$ -secretase to lipid rafts by GPI anchor addition up-regulates  $\beta$ -site processing of the amyloid precursor protein. *Proc. Natl. Acad. Sci. U.S.A.* **100**, 11735–11740
  40. Vetrivel, K. S., Cheng, H., Lin, W., Sakurai, T., Li, T., Nukina, N., Wong, P. C., Xu, H., and Thinakaran, G. (2004) Association of  $\gamma$ -secretase with lipid rafts in post-Golgi and endosome membranes. *J. Biol. Chem.* **279**, 44945–44954
  41. Andrade, A., Sandoval, A., Oviedo, N., De Waard, M., Elias, D., and Felix, R. (2007) Proteolytic cleavage of the voltage-gated  $Ca^{2+}$  channel  $\alpha_2\delta$  subunit. Structural and functional features. *Eur. J. Neurosci.* **25**, 1705–1710